Silica condensation reaction: an *ab initio* study

J. C. G. Pereira,[a,b] C. R. A. Catlow*[a]† and G. D. Price[b]

[a] *Davy Faraday Research Laboratory, The Royal Institution of Great Britain, 21 Albermarle Street, London, UK W1X 4BS*
[b] *University College London, Department of Geological Sciences, Gower Street, London, UK WC1E 6BT*

***Ab initio* techniques are used to investigate the mechanisms and energetics of condensation of two $Si(OH)_4$ monomers in a simulated hydrated environment; the calculated activation energies accord well with those measured for silica condensation in sol–gel systems.**

The kinetics of the silica-based condensation reaction have been widely investigated, using a variety of spectroscopies and scattering techniques.[1] Silicate clusters in solution have also been identified[2,3] using NMR and gas chromatographic techniques. However, because of the multitude of simultaneous reactions in solution, it is difficult to extract information about individual events using only experimental data.

The chemistry of silica has also been studied extensively using theoretical techniques.[4] A simple mechanism for the silica hydrolysis reaction was suggested,[5] with an activation energy of 21.9 kcal mol^{-1}, close to the experimental energy barrier for silicate and quartz dissolution. All these calculations were carried out in the gas phase, ignoring hydration effects. Moreover, no systematic *ab initio* studies of the silica condensation reaction have been reported to date, even for gas phase systems.

We have therefore studied the simplest condensation reaction, $2Si(OH)_4 \rightarrow Si_2O(OH)_6 + H_2O$, using DF theory coupled with a continuum dielectric model, COSMO,[6,7] to describe the electrostatic conditions found in real silica solutions. This conductor-like screening model is a continuum dielectric model, where a solute molecule is embedded in a dielectric continuum of permittivity ε. The interface between the cavity formed by the solute and the dielectric, the solvent accessible surface, has thus a surface charge distribution, arising from the polarisation of the dielectric medium in response to the charge distribution of the solute. The COSMO model calculates the screening charges in a conductor ($e = \infty$), for arbitrarily shaped cavities, using a non-iterative procedure, and then the dielectric screening energy and its gradient are scaled by $(\varepsilon - 1)/(\varepsilon + \frac{1}{2})$, to take into account the effect of the dielectric.

All calculations used the DMOL code[8] with the local BLYP functional[9,10] and a DNP double numerical basis set.[11] All atomic arrangements were first optimised *in vacuo* and subsequently recalculated including hydration effects, as a single energy point, without reoptimisation. We considered mechanisms effected by acid catalysis (corresponding to pH $<$ 3) as in most experimental work.[12,13] A methanol environment was chosen for the COSMO calculations, to fit better the electrostatic conditions found in real sol–gel solutions, where the alcohol is usually the main component. Typical compositions are water/alkoxide = 2–4 and alcohol/alkoxide = 4–10.

Acid catalysed condensation reactions are effected by the attack of a neutral monomer on a protonated monomer resulting in a protonated dimer and a water molecule; $Si(OH)_4H^+$ and $Si_2OH(OH)_6^+$ are therefore key species in the condensation reaction. The protonation energy for both clusters, presented in Table 1, shows that this process is exothermic in the gas phase and endothermic in the methanol environment. In addition, we find that it is more energetically favourable to protonate the cluster rather than the monomer. In gas phase calculations, the key factor is always the additional charge, which may generally be delocalised more effectively in larger systems; consequently, the side of the equilibrium where the charge is hosted by a larger species tends to have a lower energy. In the solvated medium, simulated by the COSMO methodology, this charge stabilisation effect is drastically reduced: it now requires more energy to protonate the $Si_2O(OH)_2$ dimer than the $Si(OH)_4$ monomer. As the electron-withdrawing effect of OSi groups is greater than that of OH groups,[1] the bridging O in $Si_2O(OH)_6$ is less basic than the four terminal O in $Si(OH)_4$. The general implication of this effect is that in acid conditions, larger neutral species attack the smaller, protonated monomers, as observed.[12]

Protonated species formation	
$Si(OH)_4 + H_3O^+ + \Delta E \rightarrow Si(OH)_3(H_2O)^+ + H_2O$	
without hydration	$\Delta E = -18.8$
with hydration	$\Delta E = +7.4$
$Si_2O(OH)_6 + H_3O^+ + \Delta E \rightarrow Si_2OH(OH)_6^+ + H_2O$	
without hydration	$\Delta E = -22.3$
with hydration	$\Delta E = +12.9$

Table 1 Formation energies, *in vacuo* and methanol environments

The energy for the condensation reaction, from the protonated reactants to the protonated products, is presented in Table 2. The results for the reaction in the gas phase are again dominated by the effects of charge distribution. The energy of the condensation reaction is negative, because the dimer is larger than the monomer. In the solvated environment, where these charge effects are relatively unimportant, the reaction is endothermic, essentially because the products have groups that are more electron withdrawing than those of the reactants. The results for the calculations with a solvated environment agree with the trends predicted experimentally for these clusters in solution.[12]

Protonated species reactions	
$Si(OH)_4 + Si(OH)_3(H_2O)^+ + \Delta E \rightarrow Si_2OH(OH)_6^+ + H_2O$	
without hydration	$\Delta E = -6.3$
with hydration	$\Delta E = +5.1$

Table 2 Condensation energy, *in vacuo* and methanol environments

We now study two detailed mechanisms of condensation: the S_N2 attack (illustrated in Fig. 1) in which the attack occurs from the opposite side to the leaving group and the lateral attack (Fig. 2) in which the attack occurs sideways. To ensure that the energy surface for the reaction was adequately searched we performed, in each case, two sets of calculations. In the first, we started from the reactants, with the protonated monomer having its equilibrium $Si–O^+$ distance of 1.88 Å. During the course of the reaction, the distance, *d*, between the oxygen of the attacking monomer and the Si of the protonated monomer was reduced in a succession of steps from *ca.* 8 Å to the equilibrium value (for the protonated dimer) of 1.83 Å; at each step along the path, *d* was held fixed and all other parameters were optimised. In the second set of calculations, we started from the products, with the protonated dimer having its equilibrium $O^+–Si$ distance of 1.83 Å. We successively decreased the distance, *d′*, between the oxygen of the leaving water molecule and the Si of the

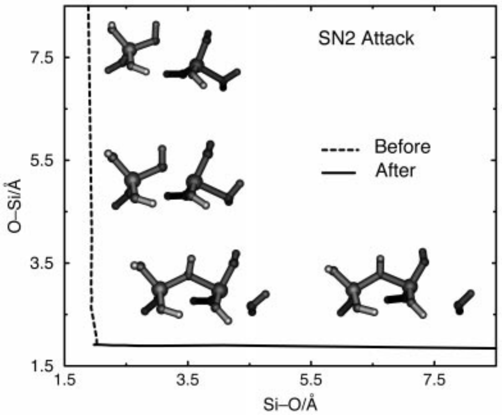

Fig. 1 S_N2 mechanism for the condensation reaction $Si(OH)_4 + Si(OH)_4H^+ \rightarrow Si_2OH(OH)_6^+ + H_2O$. The *y* axis represents the oxygen–silicon distance, (O–Si), between the attacking monomer and the protonated monomer; the *x* axis represents the silicon–oxygen distance, (Si–O), between the protonated dimer and the departing water molecule.

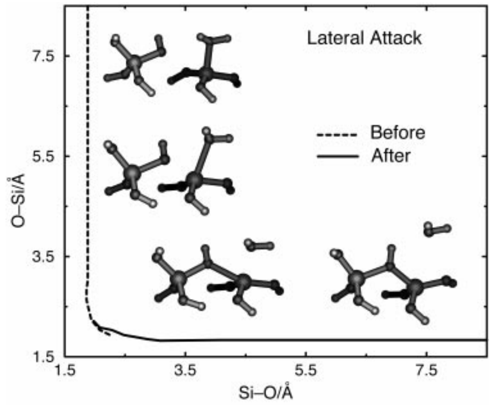

Fig. 2 Lateral attack mechanism for the condensation reaction $Si(OH)_4 + Si(OH)_4H^+ \rightarrow Si_2O(OH)_6H^+ + H_2O$. The *x* and *y* axes are as in Fig. 1.

protonated dimer, from a value of *ca.* 8 Å to the equilibrium value (for the protonated monomer) of 1.88 Å. Again *d′* was fixed in the individual calculations, with all other parameters being optimised. The two sets of calculations, denoted 'before' and 'after', result in similar energy profiles in the intermediate region where they overlap. We note that this step-by-step analysis gives valuable information about the evolution of the charge distribution, which is fundamental in understanding the full transformation from the reactants to the products.

The S_N2 and lateral attack reaction paths, optimised in the gas phase, are very different. While the S_N2 path is composed of two almost straight lines, suggesting a negligible activation energy, the lateral attack path exhibits a small energy barrier.

In the solvated environment, simulated by the COSMO methodology, the energy evolution along the S_N2 reaction path shows first a small energy barrier of 2.5 kcal mol^{-1} before decreasing to a five-silicon intermediate, which is 3.4 kcal mol^{-1} more stable than the reactants, with O–Si 1.91 Å and Si–O 1.98 Å. A second energy barrier of 11.3 kcal mol^{-1}, the largest in the whole reaction process, occurs later, when the Si–O distance is already 4.08 Å.

In the lateral attack mechanism in the solvated environment, after the first 2.5 kcal mol^{-1} energy barrier, a five-coordinate silicon intermediate occurs at O–Si 2.83 Å and Si–O 1.86 (1.9 kcal mol^{-1} less stable than the other reactants). As in the gas phase, a pronounced peak occurs at Si–O 2.48 Å, forming the largest energy barrier in the overall mechanism: 17.3 kcal mol^{-1} (6 kcal mol^{-1} larger than in the S_N2 mechanism). The S_N2 mechanism seems therefore to be an easier route for the conversion of the reactants into the products. However, as the study for the lateral attack shows, several other mechanisms that are energetically and statistically less favourable, should still be possible and may occur simultaneously in the solution.

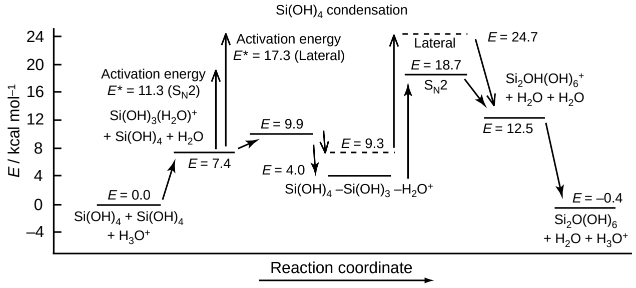

Fig. 3 Energy evolution (kcal mol^{-1}) during the $Si(OH)_4$ condensation reaction, for both S_N2 and lateral attack mechanisms

The global energy evolution from the neutral reactants to the neutral products is depicted in Fig. 3. The difference in energy between reactants and products is small: only −0.4 kcal mol^{-1}. On fully optimising both reactants and products in the COSMO environment, this difference increases to −3.2 kcal mol^{-1}, which is still relatively small. Most significant, however, is the fact that our calculated activation energies are within the range of those measured experimentally for silica condensation reactions in sol–gel systems, in the range 12–15 kcal mol^{-1}.[14,15] We may be confident therefore that we have identified the main mechanisms for this crucially important process. Further calculations will explore stabilities and condensation mechanisms for larger clusters.

We are very grateful to EPSRC for providing both local and national computer resources. One of us (J. C. G. P.) is greatly indebted to Instituto Superior Técnico, Dept. Eng. Materials, Lisboa, and JNICT, Programa Ciência and Programa Praxis XXI, Lisboa, for financial support.

Notes and References

† E-mail: richard@ri.ac.uk

1 J.-C. Pouxviel and J. P. Boilot, in *Better Ceramics Through Chemistry III*, ed. C. J. Brinker, D. E. Clark and D. R. Ulrich, Materials Research Society, Elsevier, 1986, vol. 121, p. 37; I. Artaki, M. Bradley, T. W. Zerda, J. Jonas, G. Orcel and L. L. Hench, in *Science of Ceramic Chemical Processing*, ed. L. L. Hench and D. R. Ulrich, Wiley, 1986, p. 73; C. W. Turner and C. J. Franklin, in *Science of Ceramic Processing*, ed. L. L. Hench and D. R. Ulrich, Wiley, 1986, p. 81; K. D. Keefer, in *Better Ceramics Through Chemistry*, ed. C. J. Brinker, D. E. Clark and D. R. Ulrich, Elsevier, 1984, vol. 32, p. 15.

2 L. W. Kelts and N. J. Armstrong, *J. Mater. Res.*, 1989, **4**, 423.

3 W. G. Klemperer and S. D. Ramamurthi, in *Fifth International Workshop on Glasses and Glass Ceramics from Gels*, ed. M. A. Aegerter; *J. Non-Cryst. Solids*, 1990, **121**, 16.

4 L. P. David, L. W. Burgraff and M. S. Gordon, *J. Am. Chem. Soc.*, 1988, **110**, 3056; J. Hill and J. Sauer, *J. Phys. C: Solid State Phys.*, 1994, **98**, 1238; I. Pápai, A. Goursot and F. Fajula, *J. Phys. C: Solid State Phys.*, 1994, **98**, 4654; J. A. Pople, *Ab Initio Molecular Orbital Theory*, Wiley, New York, 1986; R. G. Parr and W. Wang, *Density Functional Theory of Atoms and Molecules*, OUP, Oxford, 1989.

5 A. C. Lasaga and G. Gibbs, *Am. J. Sci.*, 1990, **290**, 263.

6 A. Klamt and G. Schüürmann, *J. Chem. Soc., Perkins Trans. 2*, 1993, 799.

7 J. Andzelm and C. Kölmel, *J. Chem. Phys*., 1995, **103**, 9312.

8 DMOL Manual, Molecular Simulations Inc., 9685 Scranton Road, San Diego, CA, 1966.

9 A. D. Becke, *Phys. Rev. A*, 1988, **3**, 3098.

10 C. Lee, W. Yang and R. G. Parr, *Phys. Rev. B*, 1988, **37**, 785.

11 B. Delley, *J. Chem. Phys.*, 1990, **92**, 508.

12 C. J. Brinker and G. W. Scherer, *Sol–Gel Science: The Physics and Chemistry of Sol–Gel Processing*, Academic Press, London, 1989.

13 R. K. Iler, *The Chemistry of Silica*, Wiley, 1979.

14 L. W. Burggraf, L. P. Davies and M. S. Gordon, in *Ultrastructure Processing of Advanced Materials*, ed. D. R. Uhlmann and D. R. Ulrich, Wiley, 1992, p. 47.

15 S. H. Garofalini and G. Martin, *J. Phys. C: Solid State Phys*., 1994, **98**, 1311.

Received in Cambridge, UK, 5th March 1988; 8/01816B